



HAL
open science

Hypoxia regulates CD9 expression and dissemination of B lymphoblasts

Jérémie Rouger-Gaudichon, Elie Cousin, Helene Jakobczyk, Lydie Debaize, Anne-Gäelle Rio, Anne Forestier, Marie-Pierre Arnaud, Arnaud Villacreces, Vincent Praloran, Rodrigo Jacamo, et al.

► **To cite this version:**

Jérémie Rouger-Gaudichon, Elie Cousin, Helene Jakobczyk, Lydie Debaize, Anne-Gäelle Rio, et al.. Hypoxia regulates CD9 expression and dissemination of B lymphoblasts. *Leukemia Research*, 2022, 123, pp.106964. 10.1016/j.leukres.2022.106964 . hal-03888260

HAL Id: hal-03888260

<https://hal.science/hal-03888260>

Submitted on 28 Feb 2023

HAL is a multi-disciplinary open access archive for the deposit and dissemination of scientific research documents, whether they are published or not. The documents may come from teaching and research institutions in France or abroad, or from public or private research centers.

L'archive ouverte pluridisciplinaire **HAL**, est destinée au dépôt et à la diffusion de documents scientifiques de niveau recherche, publiés ou non, émanant des établissements d'enseignement et de recherche français ou étrangers, des laboratoires publics ou privés.



Distributed under a Creative Commons Attribution - NonCommercial 4.0 International License

Hypoxia regulates CD9 expression and dissemination of B lymphoblasts

Short running title: Hypoxia and CD9 in ALL Cells

Jérémie Rouger-Gaudichon^{1,2*}, Elie Cousin^{1,3}, Hélène Jakobczyk¹, Lydie Debaize¹, , Anne-Gaëlle Rio¹, Anne Forestier¹, Marie-Pierre Arnaud¹, Arnaud Villacreces⁴, Vincent Praloran⁴, Rodrigo Jacamo⁵, Marie-Dominique Galibert^{1,6}, Marie-Bérengère Troadec^{1,7,8} and Virginie Gandemer^{1,3}.

¹Univ Rennes, CNRS, IGDR (Institut de Génétique et Développement de Rennes) - UMR 6290, Equipe Expression des Gènes et Oncogenèse, Rennes, France.

²University hospital, Caen, Department of Pediatric Oncology and Hematology, CHU Caen Normandie, France

³University Hospital, Rennes, Pediatric Oncology and Hematology, CHU Rennes, France

⁴Univ. Bordeaux, INSERM, BMGIC, U1035, F33000, Bordeaux, France

⁵Department of Leukemia, Section of Molecular Hematology and Therapy, The University of Texas MD Anderson Cancer Center, Houston, TX, USA.

⁶University Hospital, Rennes, Department of Molecular Genetics and Genomic, CHU Rennes, France

⁷Univ Brest, Inserm, EFS, UMR 1078, GGB, F29200 Brest, France

⁸CHRU Brest, Service de génétique, laboratoire de génétique chromosomique, Brest, France

*Correspondence: rouger-j@chu-caen.fr; Tel.: +33-02-31-06-44-88 fax: +33-02-31-49-30

Abstract:

Acute lymphoblastic leukemias (ALL) are the most frequent cancer in children and derive most often from B-cell precursors. Current survival rates roughly reach 90% at 10 years from diagnosis. However, 15-20% of children still relapse with a significant risk of death. Our previous work showed that the transmembrane protein CD9 plays a major role in lymphoblasts migration into sanctuary sites, especially in testis, through the activation of RAC1 signaling upon blasts stimulation with C-X-C chemokine ligand 12 (CXCL12). Here, we identified common factors shared by the bone marrow and extramedullary niches which could upregulate CD9 expression and function. We found that low oxygen levels

enhance CD9 expression both at mRNA and protein levels. We further determined that Hypoxia Inducible Factor 1 α (HIF1 α), the master transcription factor involved in hypoxia response, binds directly CD9 promoter and induce CD9 transcription. We also showed that CD9 protein is crucial for leukemic cell adhesion and migration at low oxygen levels, possibly through its action on RAC1 signaling. Mouse xenograft experiments indicate that HIF1 α signaling pathway promotes ALL cells dissemination in a CD9-dependent manner. The present work increments our understanding of CD9 implication in ALL pathogenesis.

Keywords:

acute lymphoblastic leukemia; children; tetraspanin; CD9; hypoxia

Introduction

Approximately 15% of children relapse from acute lymphoblastic leukemia (ALL)[1]. Most relapses occur in the bone marrow (BM), but extramedullary relapses, such as those of the testes or central nervous system, account for approximately 15% of pediatric B-ALL relapses[1–3]. It was shown that leukemic cells can migrate into these sites during early stages of the disease[4], where some remain initially in quiescence and are relatively protected from chemotherapy[5]. Hence, after treatment, either the initial leukemic clone (chemoresistant) or a leukemic clone derived from a common ancestor[6] may give rise to a relapse. We decided to address the issue of lymphoblast dissemination with the aim of preventing relapses. Following our previous work, showing that the CD9 transmembrane protein is differentially expressed in ETV6-RUNX1 B-ALL[7,8], we demonstrated that CD9 promotes leukemic cell migration into CXCL12-containing tissues, such as the testes, one of the major extramedullary sites of relapse, through activation of the RAC1 signaling pathway[9]. CD9 belongs to the tetraspanin superfamily and is involved in cell migration and adhesion of several cancers, including leukemia[10]. Here, we specifically focused on the regulation of CD9 expression. BM and extramedullary niches, such as the testes, share low oxygen (O₂) conditions[11–13]. We thus hypothesized that hypoxia may regulate CD9 expression and subsequently control cell dissemination.

Material and Methods*Cell lines and patients' cells*

The human REH cell line (ATCC® CRL-8286TM) is a pre-B ALL cell line initiated from the peripheral blood of a patient with pre-B acute lymphoid leukemia ALL in first relapse. REH

cells carry the chromosomal translocation t(12;21) and chromosomal deletion del(12) producing respective *ETV6-RUNX1* fusion gene and deletion of residual *ETV6* gene. 501-mel cell line is a melanoma cell line derived from a lymph node metastasis of a patient, and which presents the V600E mutation in the *BRAF* gene. REH and 501-mel cells were maintained in RPMI 1640 medium (Gibco, Thermo Fisher Scientific) containing 10% heat-inactivated fetal calf serum (FCS) (Eurobio) that was supplemented with antibiotics (100 U/mL penicillin-G and 100 U/mL streptomycin, Gibco). The cells were maintained at 37°C in a humidified incubator under a 5% CO₂ atmosphere at 20% O₂. To induce hypoxia in the indicated experiments, cells were incubated in a Binder CO₂ CB160 incubator at 0.2% O₂. The human embryonic kidney cells 293 (HEK293) (ATCC® CRL-1573TM) were maintained in DMEM/10% FCS/1% antibiotics. The cells were maintained at 37°C in a humidified incubator under a 5% CO₂ atmosphere at 20% O₂. Bone marrow mononuclear cells from BCP-ALL patients were collected at diagnosis, after informed consent had been obtained, in accordance with the declaration of Helsinki. The protocol was approved by the ethic committee of Rennes Hospital (Rennes, France). Vital mononuclear cells were isolated from bone marrow by successive centrifugations through lymphocytes separation medium (Eurobio), resuspended in HP01 medium (MACO biotech) supplemented with 10 ng/mL, human IL-3 (Miltenyi Biotech), 10 ng/mL human IL-7 (Miltenyi Biotech) and 100 ng/mL human Stem Cell Factor (SCF) (Miltenyi Biotech) and cultured for 24h in 0.2% O₂ or 20% O₂ before cell lysis and RNA extraction (*cf.* below).

Chemicals and plasmid vectors

DiMethylOxalyGlicine (DMOG) was purchased to Cayman Chemical (#71210). DiMethyl SulfOxyde (DMSO) was purchased to Sigma-Aldrich. Lentiviral vector bearing MISSION *pLKO.1 shRNA-puro* constructs targeting human *HIF1 α* (TRCN0000003808; targeting sequence:

CCGGCCGCTGGAGACACAATCATATCTCGAGATATGATTGTGTCTCCAGCGGTTTTT) was purchased to Sigma-Aldrich. *pLVX-SV40-Neo-CD9* vector was purchased to Creative Biogene Biotechnology. *pGL4.10-luc* plasmid vector was purchased to Promega. *HA-HIF1 α P402A/P564A-pcDNA3* plasmid vector was a gift from William Kaelin (Addgene plasmid #18955). *MSCV Luciferase PGK-hygro* vector was a gift from Scott Lowe (Addgene plasmid #18782). *pLenti-CMV-Puro-DEST* (w118-1) was a gift from Eric Campeau (Addgene plasmid # 17452). *pCMV-VSV-G* was a gift from Bob Weinberg (Addgene plasmid # 8454). *p-Gag-pol* vector was kindly given by Dr. Didier Negre. The plasmid *psPAX2* was a gift from Didier Trono (Addgene plasmid # 12260).

RNA extraction, cDNA synthesis, and RT-qPCR

RNA was extracted using the NucleoSpin RNA II (Macherey Nagel) and cDNA was synthesized using High capacity cDNA RT kit (Life Technologies) according to the manufacturers' protocol. Real-time PCR was carried out in sealed 384-well microtiter plates using the SYBR Green PCR Master Mix (Applied Biosystems), according to Applied Biosystems gene amplification specifications (40 cycles of 15 sec at 95°C and 1 min at 60°C). The forward (F) and reverse (R) primers (synthesized by Eurogentec) sequences are described in Table 1. Data analysis was performed using the DDCT-method². The housekeeping gene *ABL* was used to normalize the data. The log₂ fold change of all genes of interest compared to control cells was calculated.

Immunoblotting

Cells were cultured overnight in experimental conditions as described in Figure 2. Cells were then centrifugated at 2000 rpm for 3 minutes and lysed directly in Laemmli 1X buffer. Obtained samples were then quickly sonicated to reduce viscosity and heated at 95°C for 5 minutes. The samples were subjected to sodium dodecyl sulfate polyacrylamide gel electrophoresis (SDS-PAGE), transferred to 0.45 µM nitrocellulose membranes (GE Healthcare), blocked in TBS/0.05% Tween-20 (TBST)/5% non-fat dry milk and incubated overnight at 4°C with either a specific HIF1 α (Abcam ab2185) antibody or a specific HSC70 (Santa Cruz biotechnology, sc-7298) antibody as control. The membranes were washed and incubated 1 h at room temperature in TBST/5% non-fat dry milk containing the secondary antibody. The membranes were then washed again and incubated with a chemiluminescent substrate (Immobilion Western, Millipore) before immunoblots visualization with an Amersham imager 680 (GE Healthcare Life Sciences) according to the manufacturer's instructions.

Flow cytometry

One million of indicated cells were cultured in the indicated conditions, washed in phosphate buffer saline (PBS) and stained with either an allophycocyanin (APC)-conjugated anti-CD9 specific antibody (M-L13; Becton Dickinson - BD) or an APC mouse IgG1 κ isotype control (clone MOPC-21, BD Biosciences) diluted at 1:100 in PBS supplemented with 2% FCS for 20 minutes. Cells were then washed again and resuspended in PBS. CD9 membrane expression was compared in each condition by analyzing fluorescence intensity of cells with a BD FACS Fortessa cytometer (Biosit, SFR UMS CNRS 3480 - INSERM 018, Rennes, France). Data were analyzed using BD FACSDiva Software.

Transient transfection and luciferase assay

Genomic DNA fragments derived from the human *CD9* gene promoter at -2kb (chr12: 6,198,225 – 6,198,330 from GRCh37/hg19), -3 kb (chr12: 6,197,222 – 6,197,321), -30 kb (chr12: 6,168,395 – 6,168,722) and from the human *VEGF* gene promoter at -1 kb (chr6: 43,769,130 – 43,769,349) were cloned with a minimal promoter (5'-AGACACTAGAGGGTATATAATGGAAGCTCGACTTCCAG-3') into a luciferase reporter vector (*pGL4.10-luc*; Promega) by PCR from REH genomic DNA samples. In the same way, the mutated counterparts of these fragments were generated by PCR-directed mutagenesis and cloned into *pGL4.10-luc*. Biological replicates of HEK293 cells were plated into 12-well plates and co-transfected with 0.25 µg of *pGL4.10-luc* plasmid DNA, together with 0.25 µg of *HA-HIF1α-P402A/P564A-pcDNA3*, using lipofectamine 3000 (L3000015, Invitrogen) following manufacturer's indications. *pCMV-renilla* luciferase vector was also transfected as an internal control for transfection efficiency. Forty-eight hours after transfection, cells were lysed and assayed for luciferase activity using the dual luciferase reporter system (Promega) according to the manufacturer's protocol and a LB 960 Centro luminometer (Berthold technologies).

Generation of stable cell lines

The REH^{TRE-HIF1α-ODDmut}, the REH^{shCTL}, the REH^{shCD9} and the REH^{shRAC1} were generated as previously described[9,14]. The REH^{MSCVluc} stable cell line was obtained from retroviral transduction. To produce retrovirus, HEK293 cells were co-transfected with *MSCV Luciferase PGK-hygro* and *pCMV-VSV-G* and *p-Gag-pol* vector plasmids for packaging using Lipofectamin 3000 transfection reagent (Thermo Fisher Scientific), filtered and added to REH cells with 8 µg/mL polybrene, and transduced cells were selected in medium containing 300 µg/mL hygromycin (Invivogen). The REH^{shHIF1α}, REH^{MSCVluc-shHIF1α}, REH^{shHIF1α+CD9} stable cell lines were obtained from lentiviral transduction. To produce lentivirus, HEK293 cells were co-transfected with either MISSION *pLKO.1-shHIF1α* bearing shHIF1α or *pLVX-SV40-Neo-CD9* and *pCMV-VSV-G* and *psPAX2* plasmids for packaging using Lipofectamine 3000 transfection reagent (Thermo Fisher Scientific). After 48h, supernatant was harvested, filtered and added to REH cells, REH^{shHIF1α} and REH^{MSCVluc} with 8 µg/mL polybrene. REH^{shHIF1α} cells were selected in medium containing 0.5 µg/mL puromycin (Invivogen). REH^{MSCVluc-shHIF1α} cells were selected in medium containing 0.5 µg/mL puromycin and 300 µg/mL hygromycin (Invivogen). REH^{shHIF1α+CD9} cells were selected in medium containing 0.5 µg/mL puromycin (Invivogen) and 500 µg/mL neomycin (Sigma-Aldrich).

Chromatin immunoprecipitation followed by quantitative PCR (ChIP-qPCR)

One hundred million REH cells were cultured at 2.10^6 /mL at 0.2% O₂ for 24h and fixed exactly 10 minutes in 1% formaldehyde (648336, Polysciences) PBS solution. Fixation reaction was interrupted by adding glycine 0.1 M for 1 minute. Cells were washed in PBS twice before snap freeze in liquid nitrogen. Cells were then lysed and lysates were sonicated to shear DNA to lengths between 200 and 600 base pairs and centrifuged at 10,000 g for 10 min at room temperature. The sonicated cell supernatants were diluted 6-fold in ChIP Dilution Buffer (20 mM tris-HCl pH 8.1/150 mM NaCl/0.1% triton) and then separated in two parts, precleared with 20 μ L/tube of dynabeads protein G (10004D, Invitrogen) for at least 2h and incubated overnight with either a specific rabbit polyclonal anti-HIF1 α antibody (abcam ab2185) or an unspecific rabbit polyclonal IgG antibody (15006, Sigma-Aldrich) and yeast tRNA (R5636, Sigma Aldrich). Samples were then incubated for at least 4h with 40 μ L/tube of dynabeads protein G under agitation. Beads were washed 4 times and immunoprecipitated DNA was eluted with elution buffer containing 0.1M NaHCO₃ 1% SDS solution. Protein-DNA crosslink was reversed by incubating the samples at 65°C overnight. Immunoprecipitated DNA was then purified and processed in qPCR with specific primers targeting genomic regions as indicated (Table 1).

Migration assays

Two million alive cells that had been cultured at either 20%, 1% or 0.2% O₂ for 72h were resuspended in 100 μ L RPMI 1640 supplemented with 1% bovine serum albumin and loaded into the upper chamber of a migration system equipped with 8- μ m Transwell microporous polycarbonate membranes (Corning-Costar). We added 0.6 mL of RPMI 1640 containing 100 ng/mL of CXCL12 (Miltenyi Biotec) to the lower chamber. After 5 hours of incubation at 37°C at either 20% or 1% or 0.2% O₂, the migrated cells were subjected to trypan blue exclusion and counted. The migration rate was determined as the percentage of cells from the input that had migrated.

Adhesion assays

We coated 24-well plates with 0.1 μ g of superfibronectin diluted in PBS (Sigma-Aldrich), by incubation 2h at 37°C. Five hundred thousand cells that had been cultured at either 20%, 1% or 0.2% O₂ for 72h were resuspended in medium supplemented with 5% FCS and allowed to adhere to the fibronectin for 90 minutes at 37°C by distributing them in triplicate into the fibronectin-coated wells. Nonadherent cells were removed by thoroughly washing and wells were examined with a DMIRB Leica microscope. Images from ten randomly selected microscopic fields were acquired from each well and adherent cells were automated counts using ImageJ software.

Xenograft transplantation, bioluminescence imaging and survival analysis

NOD/scid IL2 Rg^{null} mice (Charles River Laboratories) were maintained in the ARCHE Animal Center (Biosit, SFR UMS CNRS 3480 - INSERM 018, Rennes, France) at Rennes 1 University. Animal experiments are performed after authorization from French Research Ministry, and according to European regulation. Four-week-old mice received 2 intraperitoneal injections of 20 µg/g busulfan (Busilvex; Pierre Fabre) on 2 days. They were then allowed to rest for 2 days before the IV injection of 100,000 cells as previously described[9]. For bioluminescence imaging, mice were injected with 150 mg/kg of D-luciferine (Cayman chemical) intraperitoneally before immediate counting of emitted photons with a PhotonIMAGER OPTIMA device. Dorsal luminescences were determined by quantifying photon flux through the whole mouse. Mice were imaged at the indicated time points. The general condition of the mice was monitored daily until their death. When they presented too many or too intense signs of suffering (points limit), we sacrificed them for ethical reasons.

Statistical analysis

Statistical analyses were performed with GraphPad Prism 5.0 software. Statistical significance was analyzed using nonparametric tests (Wilcoxon or Mann-Whitney), with values of $p < 0.05$ considered significant. For survival studies, Kaplan-Meier curves were generated with Prism 5 software and analyzed with Mantel-Cox tests.

Results

1. Hypoxia upregulates CD9 expression in B lymphoblasts

We collected human leukemic cells from BM at diagnosis and further cultured them for 24 hours in 20% or 0.2% oxygen. Because hematopoietic stem cells and their malignant counterparts may reside in niches where oxygen concentration is very low, we chose this low level of O₂ for illustrating our hypothesis to reproduce oxygen concentration observed in BM or sanctuary niches[11,12,15,16]. The low O₂ concentration increased CD9 mRNA levels in six of nine patient samples tested as observed for *VEGF*, the canonical marker of exposition to hypoxia condition (Figure 1A). We confirmed this result by performing similar experiments with the REH cell line, a CD9-positive B-ALL[9] cell line established from an ETV6-RUNX1-positive late relapse (Figure 1B). The expression of CD9 protein was also higher by flow cytometry in REH cells cultured in 0.2% O₂ (viability > 95%) than those cultured in 20% O₂ for 72 hours (Figure 1C), showing that hypoxia increases CD9 protein membrane expression in these cells.

2. Hypoxia-induced CD9 upregulation involves the HIF1α pathway

The transcription factor hypoxia inducible factor 1 α (HIF1 α) is the master regulator of the cellular response to hypoxia[17]. We thus modulated HIF1 α expression in our cell model using various molecular and chemical means (Supplemental Figure S1). Chemical stabilization of HIF1 α with dimethyloxalylglycine (DMOG) increased both CD9 mRNA and membrane protein expression (Figure 2 A-B). We performed experiments with the previously described REH-TRE-HIF1 α -ODDmut cell line[14], in which a stable form of HIF1 is produced upon doxycycline addition in the culture medium. Induction of an undegradable form of HIF1 α increased both CD9 mRNA levels and CD9 membrane expression (Figure 2 C-D). Conversely, downregulation of HIF1 α with a short hairpin RNA (shRNA) decreased CD9 expression, confirming that HIF1 α is involved in the regulation of CD9 expression (Figure 2 E-F).

3. *HIF1 α binds to CD9 promoter to induce its transcription*

We further asked whether HIF1 α directly regulated CD9 expression. HIF1 α dimerizes with HIF1 β under low O₂ conditions. The heterodimer translocates into the nucleus to bind chromatin at specific sequences called “hypoxia responsive elements” (HREs) and induces transcription[17]. We identified three putative HREs within the *CD9* promoter. These HRE-containing elements were cloned upstream of a luciferase reporter gene and luciferase assays were performed in the 501Mel cell line, because this cell line does not constitutively express CD9 (Figure 3A). A specific HRE-containing sequence from the *VEGF* promoter was used as a positive control (Supplemental Figure S2). Luciferase activity was lower when the HRE located -3 kb from the CD9 transcription start site was mutated (Figure 3B), suggesting that HIF1 α can bind to the CD9 promoter at this site. We confirmed the binding of HIF1 α on the -3 kb HRE by performing chromatin immunoprecipitation assays with anti-HIF1 α antibody followed by qPCR (ChIP-qPCR) in REH cultured at 0.2% O₂ or 20% O₂ (Figure 3C). Overall, these experiments show that CD9 expression is upregulated by conditions of low O₂ through the direct involvement of the HIF1 α pathway in our model.

4. *Low oxygen alters CD9-mediated adhesion and migration of lymphoblasts*

Giving that CD9 is involved in the dissemination of lymphoblasts through the RAC1 pathway[9], we next tested whether hypoxia modify CD9-related cellular adhesion and migration properties. We performed adhesion and migration assays under various O₂ culture conditions with previously described⁹ REH cells transduced with either a shRNA targeting CD9 or a non-targeted control shRNA. Our previous work showed that CD9

expression modulation did not affect cell proliferation while affecting cell adhesion and cell migration properties[9]. In the current work, adhesion was lower and the migration capacity higher under conditions of low O₂ (Figure 4A-B). In addition, CD9 was critical for cell adhesion, regardless of the O₂ level, confirming its importance for cell adhesion. Moreover, the reduction in migration resulting from CD9 under-expression was inversely proportional to the O₂ concentration. We also observed a decrease in migration rate with previously described[9] REH cells transduced with a shRNA targeting RAC1 (Figure 4C). Considering these findings with our previous results showing the role of CD9 on RAC1 activation in B lymphoblasts[9], we can hypothesize here that the RAC1 downstream signaling may be also involved in leukemic cell migration under hypoxic conditions.

5. *HIF1 α is involved in CD9-mediated migration and dissemination of lymphoblasts in vivo*

To address the role of HIF1 α in CD9-mediated leukemic cell migration, we performed migration assays with REH cells transduced with a shRNA targeting HIF1 α alone (REH shHIF1 α) or with REH shHIF1 α additionally transduced with a CD9 expression vector (REH shHIF+CD9) in 0.2% O₂. While REH shHIF1 α cells showed a lower migration rate than control, REH shHIF+CD9 cells showed a migration rate similar to control, suggesting that the role of HIF1 α in leukemic cell migration is at least partly mediated through its regulation on CD9 (Figure 5A). We further addressed the potential role of CD9 in the dissemination of leukemic cells towards hypoxic niches. We first generated REH cells to stably express luciferase and modulate HIF1 α expression at the same time. We next performed xenograft studies to assess the dissemination of leukemic cells *in vivo*, depending on level of HIF1 α expression. Our previous work showed that the lower CD9 expressed, the longer mice survived[9]. Here, HIF1 α downregulation significantly delayed leukemic cell engraftment (Figure 5B). Consequently, mice transplanted with REH shHIF1 α showed prolonged survival, but this effect was lost when mice were transplanted with REH shHIF1 α additionally transduced with a CD9 expression vector (REH shHIF1 α +CD9) (Figure 5C). These results suggest that migration and dissemination capacities of lymphoblasts in low O₂ conditions are mediated by HIF1 α signaling and CD9.

Discussion

The prognostic impact of CD9 and its role in ALL pathogenesis have previously been studied. CD9 expression has been associated with poor prognosis in B-ALL[18–20]. CD9 expression may provide stem cell properties and enhance invasion capacities of leukemic

cells into bone marrow and extramedullary tissues. In a model of Philadelphia chromosome positive acute lymphoblastic leukemia, CD9 inhibition decreased cell migration and adhesion as well as promoting apoptosis and increasing sensitivity to imatinib[21]. CD9 inhibition with specific antibodies in mice xenografted with B lymphoblasts enhanced chemosensitivity and reduced leukemic burden. Leung *et al.* showed that CD9 blockade with a specific antibody reduce leukemic testicular and leptomeningeal infiltration. The use of a CD9 specific antibody enhanced chemosensitivity of ALL cells in vitro, suppressed disease progression and was superior in combination with chemotherapy than chemotherapy alone in xenografted mice[20]. Thus, targeting CD9 appears to be an interesting therapeutic option. Better understanding CD9 role in leukemia pathogenesis and the regulation mechanisms of its expression would help to refine anti-CD9 therapeutic strategies.

In this study, we hypothesized that low O₂ as found in niches may regulate CD9 expression in lymphoblasts thereby enhancing their migration and dissemination properties. We found that low O₂ concentration upregulated CD9 expression through the activation of the HIF1 α pathway in B-ALL lymphoblasts. HIF1 α directly bound to CD9 promoter at – 3 kb from the transcription start site to induce its transcription. We also found that CD9 protein is critical for leukemic cell migration and adhesion under conditions of low O₂. Our results further suggest that CD9-mediated leukemic cell engraftment is favored by hypoxia in vivo.

The potential role of hypoxia on CD9 expression regulation has been poorly studied so far. However, our results contrast with those obtained with normal keratinocytes in which hypoxia downregulated CD9 expression through the p38/MAPK signaling pathway[22]. An other tetraspanin, CD151, was found downregulated by low oxygen conditions through the direct binding of HIF1 α on CD151 promoter in a colon carcinoma model[23]. These discrepancies may be explained by the use of different study models and suggest that the regulation of CD9 expression is a complex phenomenon depending on several factors including cellular context and microenvironmental factors.

Our previous work demonstrated that CD9 is differentially underexpressed in ETV6-RUNX1 B-ALL cells[8]. ETV6-RUNX1 B-ALL tends to relapse late in the testicular extramedullary sites[24], where oxygen content is low[13]. Since our subsequent work showed that the more CD9 expressed, the more ETV6-RUNX1 B-ALL cells migrate and adhere[9], we hypothesized that low O₂ may upregulate CD9 expression, which may favor blast cells migration and local retention in hypoxic tissues like testis. Once settled, leukemic cells may become quiescent for a long time and then be responsible for late

relapse. Indeed, hypoxia promotes quiescence of hematopoietic progenitor cells and enhance B lymphoid development[25]. Furthermore, BM microenvironment favors quiescence and chemoresistance of ALL cells by changing their gene expression profile, notably with upregulation of genes involved in the hypoxia signaling pathway and cell adhesion[26,27]. Here, our results show that low O₂ levels regulate CD9 expression through HIF1 α signaling and favor leukemic cell migration and engraftment in an ALL model. As hypoxia regulates the expression of hundreds of genes, we wondered whether the phenotype observed in our experiments could also be explained by the effects of low O₂ on targets other than CD9. For instance, two independent works suggested that *VEGFA* may play an important role in the infiltration of CNS by ALL cells[28,29]. Nevertheless, our experiments using shRNA targeting CD9, and the rescue experiment of shHIF1 α with CD9 enforced expression, demonstrated that migration and engraftment properties of leukemic cells was altered by CD9 expression modulation.

We propose a model in which ALL blasts that express sufficient CD9 protein at the cell surface are prone to migrate to sites with low O₂ tension that express CXCL12, such as the testes. Upon binding of CXCL12 to CXCR4, CD9 activates RAC1 signaling to promote cell migration, as previously shown[8]. When O₂ levels are sufficiently low, HIF1 α is stabilized and translocates into the nucleus, where it binds to the CD9 gene promoter at -3 kb to initiate transcription (Figure 6).

Conclusion

To conclude, we propose a model in which low O₂ levels upregulate CD9 expression, promote CD9-dependent cell adhesion and migration and could promote local retention and survival. Better understanding of the role of CD9 in leukemia pathogenesis and of the regulation mechanisms of its expression would help to refine anti-CD9 therapeutic strategies, which may be beneficial in several cancer models including leukemia[20,21,30].

Acknowledgments:

The authors would like to thank all the members of Gene Expression and Oncogenesis team for insightful discussions and for providing scientific expertise. We are most grateful to the patients and patients' families of the Rennes University Hospital, CHRU Rennes. We thank the following core facilities of the BIOSIT SFR UMS CNRS 3480 - INSERM 018: Mric-Photonics (Stéphanie Dutertre), flow cytometry and cell sorting (Laurent Deleurme, Gersende Lacombe), and ARCHE animal housing (Laurence Bernard-Touami), H2P2 (Alain Fautrel). We thank the MICMAC team at INSERM UMR U1236 for kindly allowing us to perform some of our experiments in their laboratory (Pr. Karin Tarte, Frédéric Mourcin). This research was funded by the Rennes Hospital FHU CAMin (CHU de Rennes), Brittany Regional Council (Région Bretagne), comprehensive cancer Centre Eugène Marquis Cancer Care Foundation LNCC-CD35 (Ligue Contre le Cancer), Société Française de lutte contre les Cancers et leucémies de l'Enfant et de l'adolescent, Manche Leucémie association, and People Programme (Marie Curie Actions) of the European Union's Seventh Framework Programme (REA grant agreement n°291851). We are grateful to the Manche Leucémie association for their financial support.

Authorship Contributions:

“Conceptualization, J.R.G., V.G. and M.B.T.; methodology, J.R.G., V.G. and M.B.T.; formal analysis, J.R.G. E.C., A.G.R.; investigation, J.R.G., E.C., M.P.A, A.V., A.G.R., H.J, L.D., A.F.; resources, V.P., R.J., A.V.; writing—original draft preparation, J.R.G.; writing—review and editing, E.C., H.J., L.D., M.D.G., M.B.T., V.G., supervision, V.G., M.B.T., M.D.G.; funding acquisition, J.R.G., V.G. All authors have read and agreed to the published version of the manuscript.” This research was funded by the Rennes Hospital FHU CAMin (CHU de Rennes), Brittany Regional Council (Région Bretagne), comprehensive cancer Centre Eugène Marquis Cancer Care Foundation LNCC-CD35 (Ligue Contre le Cancer), Société Française de lutte contre les Cancers et leucémies de l’Enfant et de l’adolescent, Manche Leucémie association, and People Programme (Marie Curie Actions) of the European Union's Seventh Framework Programme (REA grant agreement n°291851).

Disclosure of Conflicts of Interest:

The authors declare no conflict of interest. The funders had no role in the design of the study; in the collection, analyses, or interpretation of data; in the writing of the manuscript, or in the decision to publish the results.

Journal Pre-proof

References

- [1] T. Oskarsson, S. Söderhäll, J. Arvidson, E. Forestier, S. Montgomery, M. Bottai, B. Lausen, N. Carlsen, M. Hellebostad, P. Lähteenmäki, U.M. Saarinen-Pihkala, Ó. G.Jónsson, M. Heyman, Relapsed childhood acute lymphoblastic leukemia in the Nordic countries: prognostic factors, treatment and outcome, *Haematologica*. 101 (2016) 68–76. <https://doi.org/10.3324/haematol.2015.131680>.
- [2] J. Gaudichon, H. Jakobczyk, L. Debaize, E. Cousin, M.-D. Galibert, M.-B. Troadec, V. Gandemer, Mechanisms of extramedullary relapse in acute lymphoblastic leukemia: Reconciling biological concepts and clinical issues, *Blood Rev.* 36 (2019) 40–56. <https://doi.org/10.1016/j.blre.2019.04.003>.
- [3] G. Tallen, R. Ratei, G. Mann, G. Kaspers, F. Niggli, A. Karachunsky, W. Ebell, G. Escherich, M. Schrappe, T. Klingebiel, R. Fengler, G. Henze, A. von Stackelberg, Long-Term Outcome in Children With Relapsed Acute Lymphoblastic Leukemia After Time-Point and Site-of-Relapse Stratification and Intensified Short-Course Multidrug Chemotherapy: Results of Trial ALL-REZ BFM 90, *Journal of Clinical Oncology*. 28 (2010) 2339–2347. <https://doi.org/10.1200/JCO.2009.25.1983>.
- [4] M.T.S. Williams, Y.M. Yousafzai, A. Elder, K. Rehe, S. Bomken, L. Frishman-Levy, S. Tavor, P. Sinclair, K. Dormon, D. Masic, T. Perry, V.J. Weston, P. Kearns, H. Blair, L.J. Russell, O. Heidenreich, J.A.E. Irving, S. Izraeli, J. Vormoor, G.J. Graham, C. Halsey, The ability to cross the blood–cerebrospinal fluid barrier is a generic property of acute lymphoblastic leukemia blasts, *Blood*. 127 (2016) 1998–2006. <https://doi.org/10.1182/blood-2015-08-665034>.
- [5] M.B. Meads, R.A. Gatenby, W.S. Dalton, Environment-mediated drug resistance: a major contributor to minimal residual disease, *Nature Reviews Cancer*. 9 (2009) 665–674.
- [6] F.W. van Delft, S. Horsley, S. Colman, K. Anderson, C. Bateman, H. Kempinski, J. Zuna, C. Eckert, V. Saha, L. Kearney, A. Ford, M. Greaves, Clonal origins of relapse in ETV6-RUNX1 acute lymphoblastic leukemia, *Blood*. 117 (2011) 6247–6254. <https://doi.org/10.1182/blood-2010-10-314674>.
- [7] V. Gandemer, A.-G. Rio, M. de Tayrac, V. Sibut, S. Mottier, B. Ly Sunnaram, C. Henry, A. Monnier, C. Berthou, E. Le Gall, A. Le Treut, C. Schmitt, J.-Y. Le Gall, J. Mosser, M.-D. Galibert, Five distinct biological processes and 14 differentially expressed genes characterize TEL/AML1-positive leukemia, *BMC Genomics*. 8 (2007) 385. <https://doi.org/10.1186/1471-2164-8-385>.
- [8] V. Gandemer, M. Aubry, M. Roussel, A.-G. Rio, M. de Tayrac, A. Vallee, J. Mosser, B. Ly-Sunnaram, M.-D. Galibert, CD9 expression can be used to predict childhood TEL/AML1-positive acute lymphoblastic leukemia: proposal for an accelerated diagnostic flowchart, *Leuk. Res.* 34 (2010) 430–437. <https://doi.org/10.1016/j.leukres.2009.09.033>.
- [9] M.-P. Arnaud, A. Vallée, G. Robert, J. Bonneau, C. Leroy, N. Varin-Blank, A.-G. Rio, M.-B. Troadec, M.-D. Galibert, V. Gandemer, CD9, a key actor in the dissemination of lymphoblastic leukemia, modulating CXCR4-mediated migration via RAC1 signaling, *Blood*. 126 (2015) 1802–1812. <https://doi.org/10.1182/blood-2015-02-628560>.
- [10] M. Zöller, Tetraspanins: push and pull in suppressing and promoting metastasis, *Nat. Rev. Cancer*. 9 (2009) 40–55. <https://doi.org/10.1038/nrc2543>.
- [11] J.A. Spencer, F. Ferraro, E. Roussakis, A. Klein, J. Wu, J.M. Runnels, W. Zaher, L.J. Mortensen, C. Alt, R. Turcotte, R. Yusuf, D. Côté, S.A. Vinogradov, D.T. Scadden, C.P. Lin, Direct measurement of local oxygen concentration in the bone marrow of live animals, *Nature*. 508 (2014) 269–273. <https://doi.org/10.1038/nature13034>.
- [12] Z. Ivanovic, Hypoxia or in situ normoxia: The stem cell paradigm, *J. Cell. Physiol.* 219 (2009) 271–275. <https://doi.org/10.1002/jcp.21690>.

- [13] J.G. Reyes, J.G. Farias, S. Henríquez-Olavarrieta, E. Madrid, M. Parraga, A.B. Zepeda, R.D. Moreno, The Hypoxic Testicle: Physiology and Pathophysiology, *Oxid Med Cell Longev.* 2012 (2012). <https://doi.org/10.1155/2012/929285>.
- [14] O. Frolova, I. Samudio, J.M. Benito, R. Jacamo, S.M. Kornblau, A. Markovic, W. Schober, H. Lu, Y.H. Qiu, D. Buglio, others, Regulation of HIF-1 α signaling and chemoresistance in acute lymphocytic leukemia under hypoxic conditions of the bone marrow microenvironment, *Cancer Biology & Therapy.* 13 (2012) 858–870.
- [15] A.V. Guitart, C. Debeissat, F. Hermitte, A. Villacreces, Z. Ivanovic, H. Boeuf, V. Praloran, Very low oxygen concentration (0.1%) reveals two FDCP-Mix cell subpopulations that differ by their cell cycling, differentiation and p27KIP1 expression, *Cell Death Differ.* 18 (2011) 174–182. <https://doi.org/10.1038/cdd.2010.85>.
- [16] L. Schito, S. Rey, M. Konopleva, Integration of hypoxic HIF- α signaling in blood cancers, *Oncogene.* 36 (2017) 5331–5340. <https://doi.org/10.1038/onc.2017.119>.
- [17] P. Ratcliffe, P. Koivunen, J. Myllyharju, J. Ragoussis, J.V. Bovée, I. Batinic-Haberle, C. Vinatier, V. Trichet, F. Robriquet, L. Oliver, B. Gardie, Update on hypoxia-inducible factors and hydroxylases in oxygen regulatory pathways: from physiology to therapeutics, *Hypoxia (Auckl).* 5 (2017) 11–20. <https://doi.org/10.2147/HP.S127042>.
- [18] P. Liang, M. Miao, Z. Liu, H. Wang, W. Jiang, S. Ma, C. Li, R. Hu, CD9 expression indicates a poor outcome in acute lymphoblastic leukemia, *Cancer Biomark.* (2017). <https://doi.org/10.3233/CBM-170422>.
- [19] K.T. Leung, K.Y.Y. Chan, P.C. Ng, T.K. Lau, W.M. Chiu, K.S. Tsang, C.K. Li, C.K.L. Kong, K. Li, The tetraspanin CD9 regulates migration, adhesion, and homing of human cord blood CD34+ hematopoietic stem and progenitor cells, *Blood.* 117 (2011) 1840–1850. <https://doi.org/10.1182/blood-2010-04-281329>.
- [20] K.T. Leung, C. Zhang, K.Y.Y. Chan, K. Li, J.T.K. Cheung, M.H.L. Ng, X.-B. Zhang, T. Sit, W.Y.W. Lee, W. Kang, K.F. To, J.W.S. Yu, T.K.F. Man, H. Wang, K.S. Tsang, F.W.T. Cheng, G.K.S. Lam, T.W. Chow, A.W.K. Leung, T.F. Leung, P.M.P. Yuen, P.C. Ng, C.K. Li, CD9 blockade suppresses disease progression of high-risk pediatric B-cell precursor acute lymphoblastic leukemia and enhances chemosensitivity, *Leukemia.* 34 (2020) 709–720. <https://doi.org/10.1038/s41375-019-0593-7>.
- [21] C. Xing, W. Xu, Y. Shi, B. Zhou, D. Wu, B. Liang, Y. Zhou, S. Gao, J. Feng, CD9 knockdown suppresses cell proliferation, adhesion, migration and invasion, while promoting apoptosis and the efficacy of chemotherapeutic drugs and imatinib in Ph+ ALL SUP-B15 cells, *Mol Med Rep.* 22 (2020) 2791–2800. <https://doi.org/10.3892/mmr.2020.11350>.
- [22] X. Jiang, X. Guo, X. Xu, M. Teng, C. Huang, D. Zhang, Q. Zhang, J. Zhang, Y. Huang, Hypoxia regulates CD9-mediated keratinocyte migration via the P38/MAPK pathway, *Sci Rep.* 4 (2014) 6304. <https://doi.org/10.1038/srep06304>.
- [23] C.-W. Chien, S.-C. Lin, Y.-Y. Lai, B.-W. Lin, S.-C. Lin, J.-C. Lee, S.-J. Tsai, Regulation of CD151 by hypoxia controls cell adhesion and metastasis in colorectal cancer, *Clin. Cancer Res.* 14 (2008) 8043–8051. <https://doi.org/10.1158/1078-0432.CCR-08-1651>.
- [24] V. Gandemer, S. Chevret, A. Petit, C. Vermylen, T. Leblanc, G. Michel, C. Schmitt, O. Lejars, P. Schneider, F. Demeocq, B. Bader-Meunier, F. Bernaudin, Y. Perel, M.-F. Auclerc, J.-M. Cayuela, G. Leverger, A. Baruchel, FRALLE Group, Excellent prognosis of late relapses of ETV6/RUNX1-positive childhood acute lymphoblastic leukemia: lessons from the FRALLE 93 protocol, *Haematologica.* 97 (2012) 1743–1750. <https://doi.org/10.3324/haematol.2011.059584>.
- [25] S. Chabi, B. Uzan, I. Naguibneva, J. Rucci, L. Fahy, J. Calvo, M.-L. Arcangeli, F. Mazurier, F. Pflumio, R. Haddad, Hypoxia Regulates Lymphoid Development of Human Hematopoietic Progenitors, *Cell Rep.* 29 (2019) 2307-2320.e6. <https://doi.org/10.1016/j.celrep.2019.10.050>.

- [26] S.L. Rellick, G. Hu, D. Piktel, K.H. Martin, W.J. Geldenhuys, R.R. Nair, L.F. Gibson, Co-culture model of B-cell acute lymphoblastic leukemia recapitulates a transcription signature of chemotherapy-refractory minimal residual disease, *Sci Rep.* 11 (2021) 15840. <https://doi.org/10.1038/s41598-021-95039-x>.
- [27] S. Ebinger, E.Z. Özdemir, C. Ziegenhain, S. Tiedt, C. Castro Alves, M. Grunert, M. Dworzak, C. Lutz, V.A. Turati, T. Enver, H.-P. Horny, K. Sotlar, S. Parekh, K. Spiekermann, W. Hiddemann, A. Schepers, B. Polzer, S. Kirsch, M. Hoffmann, B. Knapp, J. Hasenauer, H. Pfeifer, R. Panzer-Grümayer, W. Enard, O. Gires, I. Jeremias, Characterization of Rare, Dormant, and Therapy-Resistant Cells in Acute Lymphoblastic Leukemia, *Cancer Cell.* 30 (2016) 849–862. <https://doi.org/10.1016/j.ccell.2016.11.002>.
- [28] I. Kato, Y. Nishinaka, M. Nakamura, A.U. Akarca, A. Niwa, H. Ozawa, K. Yoshida, M. Mori, D. Wang, M. Morita, H. Ueno, Y. Shiozawa, Y. Shiraishi, S. Miyano, R. Gupta, K. Umeda, K. Watanabe, K. Koh, S. Adachi, T. Heike, M.K. Saito, M. Sanada, S. Ogawa, T. Marafioti, A. Watanabe, T. Nakahata, T. Enver, Hypoxic adaptation of leukemic cells infiltrating the CNS affords a therapeutic strategy targeting VEGFA, *Blood.* 129 (2017) 3126–3129. <https://doi.org/10.1182/blood-2016-06-721712>.
- [29] V. Münch, L. Trentin, J. Herzig, S. Demir, F. Seyfried, J.M. Kraus, H.A. Kestler, R. Köhler, T.F.E. Barth, G. te Kronnie, K.-M. Debatin, L.H. Meyer, Central nervous system involvement in acute lymphoblastic leukemia is mediated by vascular endothelial growth factor, *Blood.* 130 (2017) 643–654. <https://doi.org/10.1182/blood-2017-03-769315>.
- [30] T. Suwatthanarak, M. Tanaka, Y. Miyamoto, K. Miyado, M. Okochi, Inhibition of cancer-cell migration by tetraspanin CD9-binding peptide, *Chem Commun (Camb).* 57 (2021) 4906–4909. <https://doi.org/10.1039/d1cc01295a>.

Figure Legends

Figure 1. Low oxygen upregulates CD9 expression. A. Low oxygen (O₂) increases CD9 mRNA levels in leukemia cells from patients. Bone marrow childhood B-ALL cells were collected at diagnosis and cultured either in 20% or 0.2% O₂ for 24 h before RNA extraction, reverse transcription, and analysis by quantitative PCR. VEGF was used as a positive control. Bars represent the mean +/- standard error of the mean (SE). **B.** Low O₂ increases CD9 mRNA levels in an ETV6-RUNX1 positive REH cell line. REH cells were cultured in 20% or 0.2% oxygen for 24 h. Relative CD9 mRNA levels are shown and compared to those of EGFL7 (negative control) and VEGF and CXCR4 (positive controls). Bars represent the mean value of at least four independent experiments +/- SE and each dot represents one experiment. *p < 0.05, **p < 0.01, ***p < 0.001 by the Wilcoxon test, NS = non-statistically significant. **C.** Low O₂ increases CD9 surface expression in the REH cell line. REH cells were cultured in 20% or 0.2% O₂ for 72 h, washed, and stained with

either allophycocyanin (APC)-conjugated anti-CD9 specific antibody or a nonspecific IgG for 20 min. The cells were washed again and CD9 membrane expression assessed under each condition by flow cytometry. The mean fluorescence intensities of seven independent paired experiments are shown in the dot plot. * $p < 0.05$ by a paired Wilcoxon test.

Figure 2. Hypoxia-induced CD9 upregulation involves HIF1 α . **A.** REH cells were treated with 200 μ M DMOG or 0.2% DMSO (vehicle) for 24 h at 20% O₂ before RNA extraction, reverse transcription, and analysis by quantitative PCR. Relative mRNA levels of CD9, the negative control EGFL7, and the positive controls VEGF and CXCR4 were compared. Bars represent the mean value of at least four independent experiments \pm standard error of the mean (SE) and each point represents one experiment. * $p < 0.05$, ** $p < 0.01$, *** $p < 0.001$ by the Wilcoxon test, NS = non-statistically significant. **B.** REH cells were treated with 200 μ M DMOG or 0.2% DMSO (vehicle) for 72 h at 20% O₂, washed, and stained with either an allophycocyanin (APC)-conjugated anti-CD9 specific antibody or a nonspecific IgG and analyzed by flow cytometry. Histograms show the results of a representative experiment. Mean fluorescence intensities of seven independent paired experiments are shown in the dot plot. * $p < 0.05$ by a paired Wilcoxon test. **C.** Previously described REH-TRE-HIF1 α -ODDmut was used for this experiment. Expression of an undegradable form of HIF1 α was induced by treating the cells with 1 μ g/L doxycycline for 24 h at 20% O₂ before RNA extraction, reverse transcription, and analysis by qPCR. Relative mRNA levels of CD9, the negative control EGFL7, and the positive controls VEGF and CXCR4 were compared. Bars represent the mean value of at least three independent experiments \pm SE and each point represents one experiment. * $p < 0.05$, ** $p < 0.01$, *** $p < 0.001$ by the Wilcoxon test, NS = non-statistically significant. **D.** Expression of an undegradable form of HIF1 α was induced by treating REH-TRE-HIF1 α -ODDmut cells with 1 μ g/L doxycycline for 72 h at 20% O₂ and the cells were washed and stained with either an APC-conjugated anti-CD9 specific antibody or a nonspecific IgG and analyzed by flow cytometry. Histograms show the result of a representative experiment. Mean fluorescence intensities of seven independent paired experiments are shown in the dot plot. ** $p < 0.01$ by a paired Wilcoxon test. **E.** Downregulation of HIF1 α decreases CD9 mRNA levels by REH cells. RNA extraction, reverse transcription, and analysis by quantitative PCR were performed on REH cells transduced with either a shRNA targeting HIF1 α or a nonspecific shRNA (CTL). Relative mRNA levels of CD9, the negative control EGFL7, and the positive controls VEGF and CXCR4 were compared. Bars represent the mean value of at least three independent experiments \pm SE and each point represents one experiment. **F.** REH

cells transduced with either a shRNA targeting HIF1 α or a nonspecific shRNA (CTL) were washed and stained with either an APC-conjugated anti-CD9 specific antibody or a nonspecific IgG and analyzed by flow cytometry. Histograms show the results of a representative experiment. Mean fluorescence intensities of five independent paired experiments are shown in the dot plot. ** $p < 0.01$ by a paired Wilcoxon test.

Figure 3. HIF1 α binds to CD9 promoter. A. Scheme of plasmid constructs used in Figure 3B. Three boxes representing hypoxia-responsive elements (HRE) are shown upstream of the CD9 transcription initiation site and the mutated HRE-containing fragment of the CD9 promoter is shown in red (native HRE in yellow). **B.** Luciferase assays performed with a plasmid vector encoding an undegradable form of HIF1 α in the 501-mel cell line suggest HIF1 α binding to the CD9 promoter at -3 kb. Bars represent the mean value of luciferase levels (firefly luciferase/renilla luciferase) from at least four independent experiments +/- SE and each point represents one experiment and the mean of three replicates. ** $p < 0.01$ by the Wilcoxon test, NS = non-statistically significant. **C.** Chromatin immunoprecipitation using specific anti-HIF1 α antibodies followed by qPCR (ChIP-qPCR) in REH cells cultured at 20% or 0.2% O₂ confirms HIF1 α binding to the CD9 promoter. Bars represent the mean +/- SE of at least three independent experiments.

Figure 4. Low O₂ alters CD9-mediated adhesion and migration of lymphoblasts. A. Low O₂ and CD9 downregulation impair adhesion of the REH leukemic cell line. REH cells expressing either a control (CTL) shRNA or specific CD9 shRNA were cultured in 20%, 1%, or 0.2% O₂ for 72 h and further seeded onto superfibronectin-coated 96-well plates to adhere for 90 min in 20%, 1%, or 0.2% O₂. Adherent cells were counted using ImageJ software. Each dot represents the count obtained for one well. Bars represent the mean value of at least three independent experiments +/- SE. * $p < 0.05$, ** $p < 0.01$, *** $p < 0.001$ by the Wilcoxon test, NS = non-statistically significant. **B.** Low O₂ increases CD9-dependent migration of the REH leukemic cell line. REH cells expressing either a control (CTL) shRNA or specific CD9 shRNA were cultured in 20%, 1%, or 0.2% O₂ for 72 h and chemotactic migration towards CXCL12 measured for alive cells in a Boyden chamber for 5 h in 20%, 1%, or 0.2% O₂. The migration rate was determined by calculating the ratio between the total number of seeded cells and that of the migrating cells. Each dot represents the count obtained for one well. Bars represent the mean value of at least three independent experiments +/- SE. * $p < 0.05$, ** $p < 0.01$, *** $p < 0.001$ by the Wilcoxon test, NS = non-statistically significant. **C.** Low O₂ increases RAC1-dependent migration of the

REH leukemic cell line. Same experiment as in Figure 4B was performed with REH cells expressing either a control (CTL) shRNA or a specific RAC1 shRNA cultured in 20%, 1%, or 0.2% O₂. Each dot represents the count obtained for one well. Bars represent the mean value of at least three independent experiments +/- SE. *p < 0.05, **p < 0.01, ***p < 0.001 by the Wilcoxon test, NS = non-statistically significant.

Figure 5. HIF1 α is involved in migration and dissemination capacities of lymphoblasts through its effects on CD9. A.

HIF1 α is involved in REH cell migration probably through its regulation on CD9 expression. REH cells expressing either a control (CTL) shRNA or a specific HIF1 α shRNA, or a specific HIF1 α shRNA and a CD9 expression vector were cultured in 0.2% O₂ for 72 h and chemotactic migration towards CXCL12 measured in a Boyden chamber for 5 h in 0.2% O₂. The migration rate was determined by calculating the ratio between the total number of seeded cells and that of the migrating cells. Each dot represents the count obtained for one well. Bars represent the mean value of at least three independent experiments +/- SE. *p < 0.05, **p < 0.01, ***p < 0.001 by the Wilcoxon test, NS = non-statistically significant.

B. HIF1 α inhibition delays ALL cell engraftment in xenografted mice. NOD/*scid* IL2 Rg^{null} mice were transplanted with either an REH cell line stably expressing luciferase alone or stably expressing both luciferase and a specific shRNA targeting HIF1 α . Engraftment was then monitored at the indicated timepoints by quantifying photon flux through the entire mouse with a photonIMAGER Optima. A representative example of an experiment is shown. The graph shows the quantification of bioluminescence measured as the number of counts per minute (cpm) per cm². Each dot represents the mean value measured for at least four mice +/- SE. All mice transplanted with the control cell line spontaneously died shortly after D21 acquisition. In the shHIF1 α subset, mice were sacrificed after the last acquisition at D31 regarding their advanced symptoms of acute leukemia. **C.** HIF1 α inhibition prolongs the survival of mice xenografted with the ALL cell line. NOD/*scid* IL2 Rg^{null} mice were transplanted with either an REH cell line stably expressing a shRNA targeting HIF1 α +/- a CD9 expression vector or a control REH cell line and mice monitored daily until sacrifice (in presence of too many signs of suffering) or spontaneous death. All mice developed signs of leukemia. Kaplan-Meier curves were plotted. Mantel-Cox tests gave a p-value < 0.05 when the shHIF1 α curve was compared with either the shHIF1 α +CD9 or control curves.

Figure 6. Proposed model for hypoxia-associated CD9 regulation and function. In this model, ALL blasts that express sufficient CD9 protein at the cell surface are prone to migrate to sites with low O₂ concentration that express CXCL12, such as the testes. Upon binding of CXCL12 to CXCR4, CD9 activates RAC1 signaling to promote cell migration, as previously shown and represented in the upper frame¹. When O₂ levels are sufficiently low, HIF1 α is stabilized and translocates into the nucleus, where it binds to the CD9 gene promoter at -3 kb to initiate transcription. In this model, low O₂ levels upregulate CD9 expression, promote CD9-dependent cell adhesion and migration and could promote local retention and survival.

Tables

Table 1. List of primers used in this study

Application	Gene	Forward	Reverse
RT-qPCR	<i>ABL</i>	CCAAGAAGGGGCTGTCCT	ATGCTACTGGCCGCTGAA
	<i>CD9</i>	CAACAAGCTGAAAACCAAGGA	CAAACCACAGCAGTTCAACG
	<i>CXCR4</i>	CTACACCGAGGAAATGGGCT	AACCCATGACCAGGATGACC
	<i>VEGF</i>	AAGGAGGAGGGCAGAATCAT	CACACAGGATGGCTTGAAGA
	<i>EGFL7</i>	TTGCCAGTCAGATGTGGATGA	CTCCCTTGGGCACACAGAGT
	<i>HIF1α</i>	TCGCATCTTGATAAGGCCTCT	GCAATTCATCTGTGCTTTCATGT
ChIP qPCR	<i>CD9_HRE_-2kb</i>	AATTCCCTCCTCCGCATTGA	AGGGAGAGATCAGAGGCAGAA
	<i>CD9_HRE_-3kb</i>	GTCTCGATCTCCTCACCTCG	AAAGCTATGCACTTCTCGGC
	<i>VEGF_HRE_-1kb</i>	AGGAACAAGGGCCTCTGTC	GTTTGTGGAGCTGAGAACGG
	<i>CXCR4_HRE_-1.3kb</i>	CCTCTCCTCGGGACCATTTCC	CTGGCTGAGGTTTGCAGTG
	<i>ETV6</i> (negative control)	GCAGGCCAACATACCCTTTA	GATGAACGGGTGCAGTTTTT

Figures

Figure 1

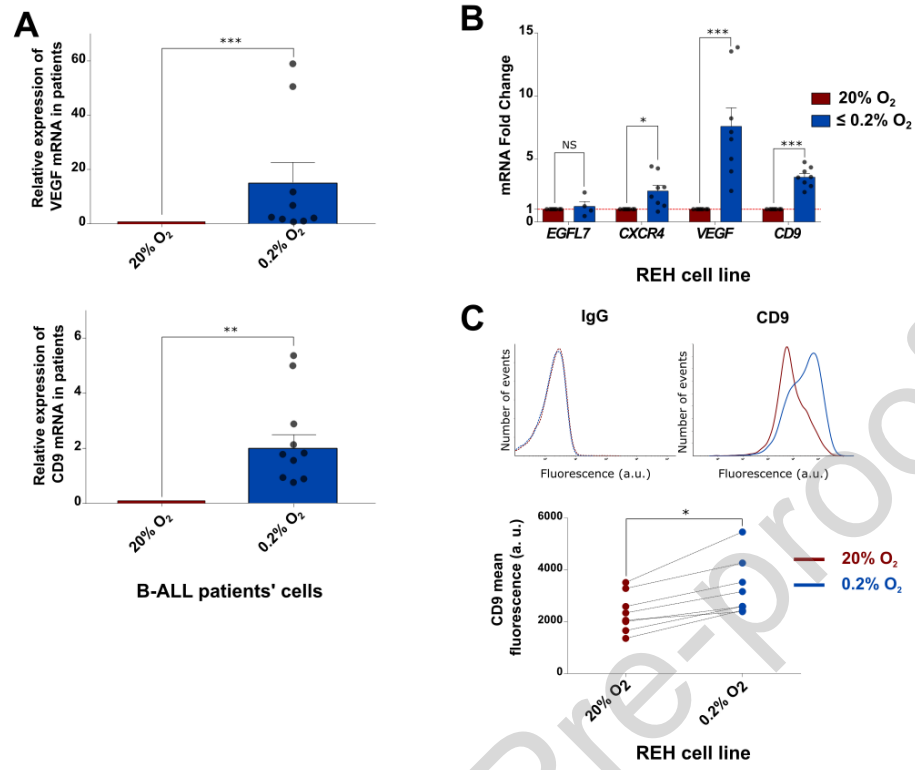


Figure 2

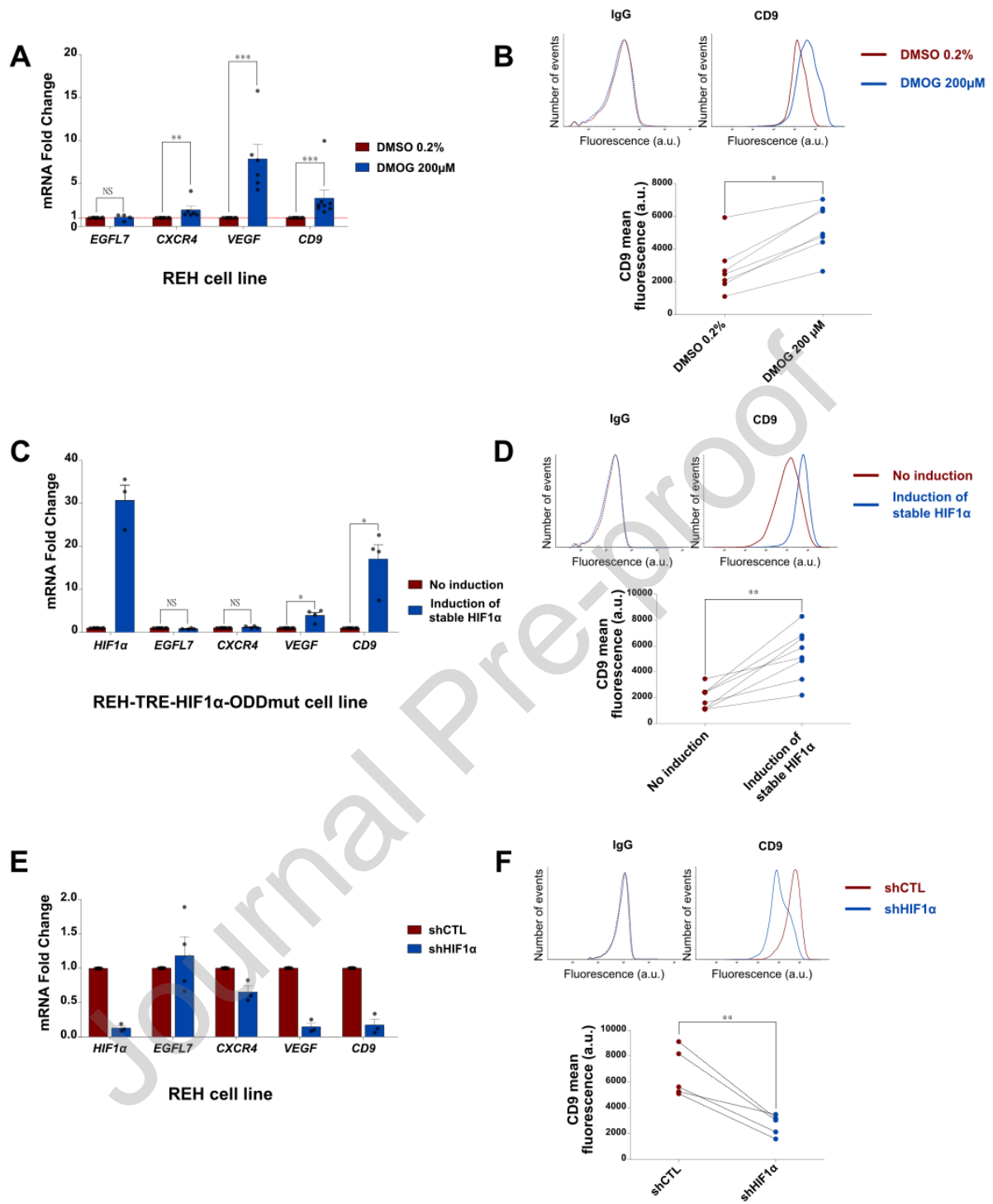


Figure 3

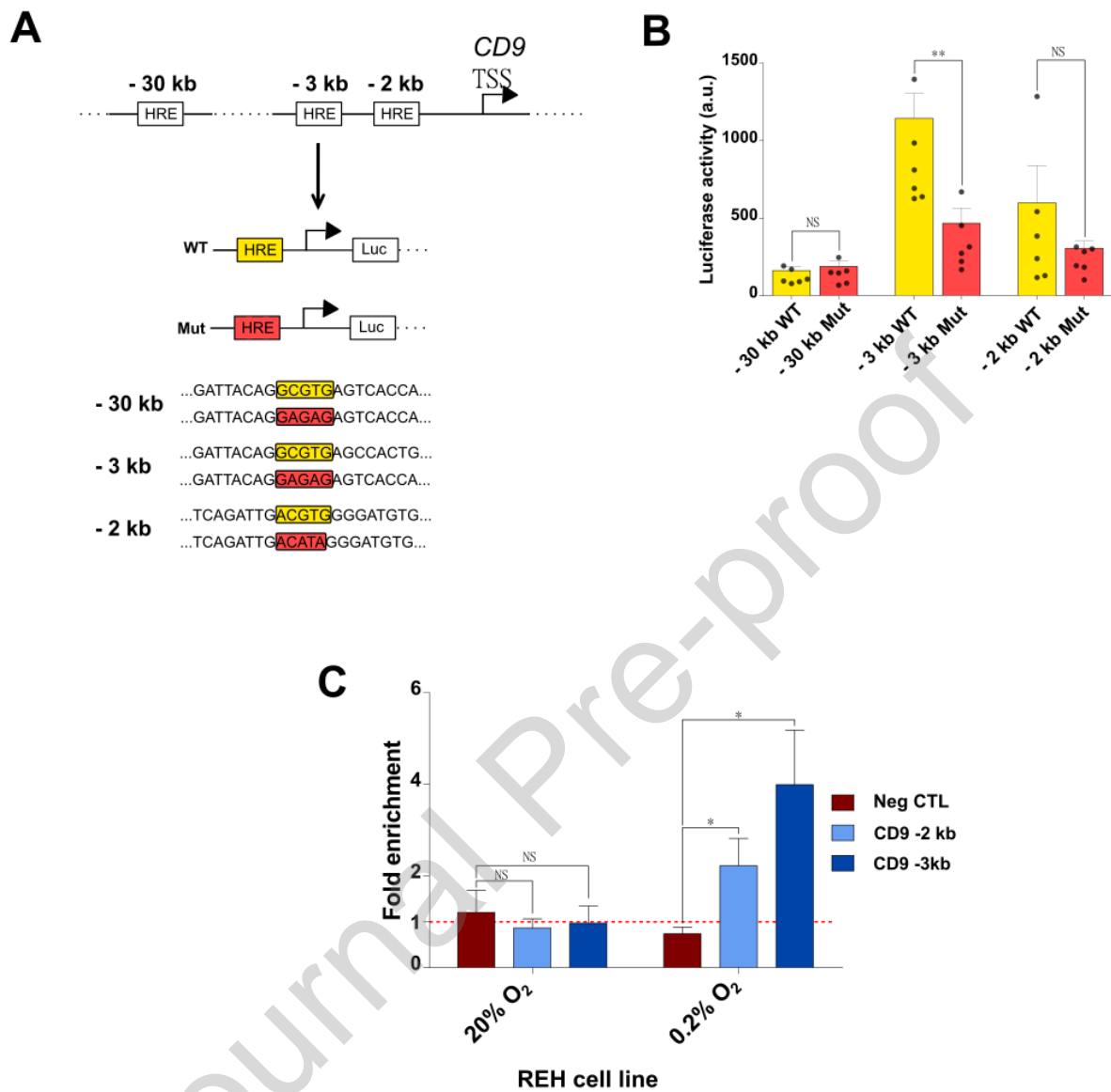


Figure 4

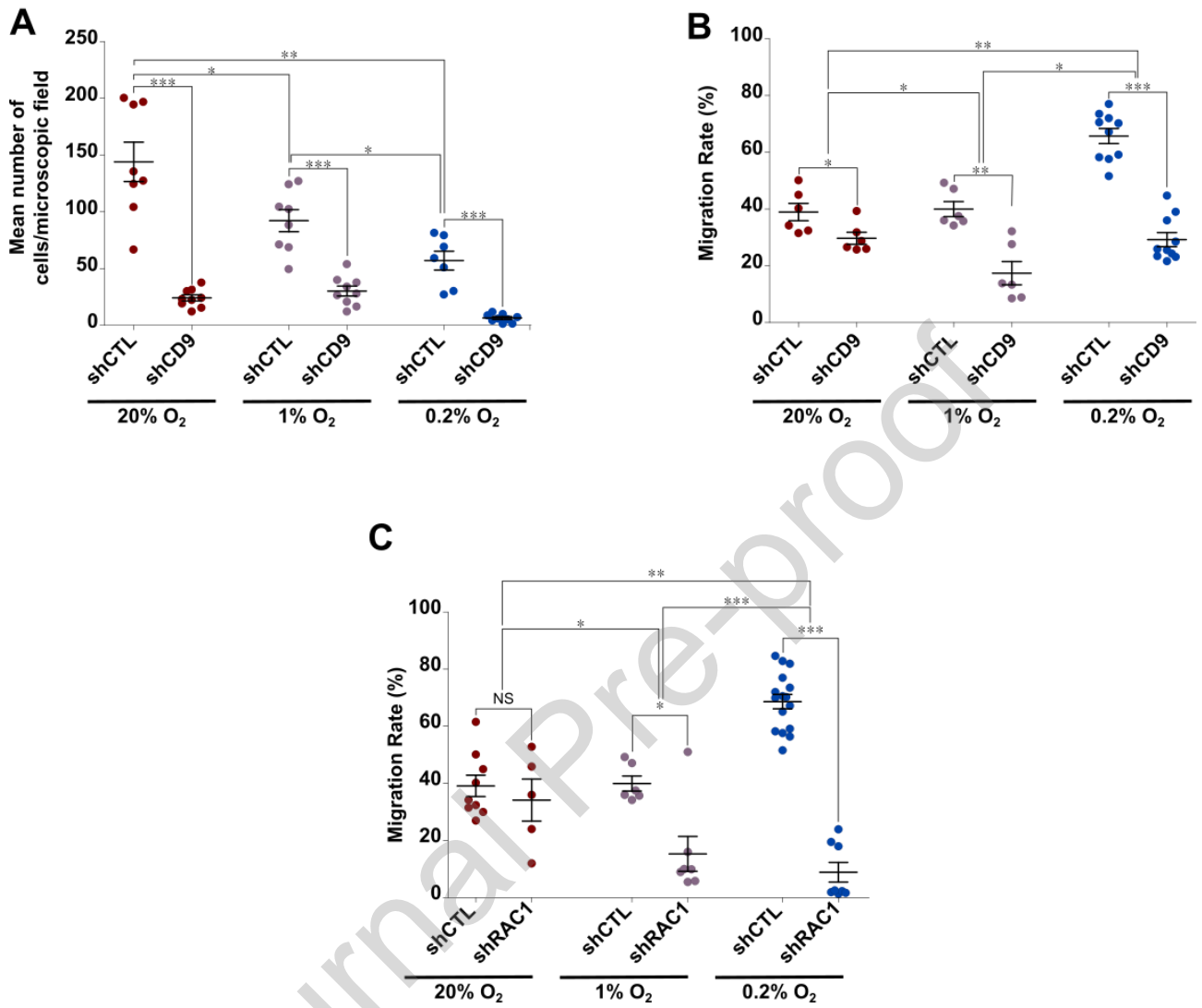


Figure 5

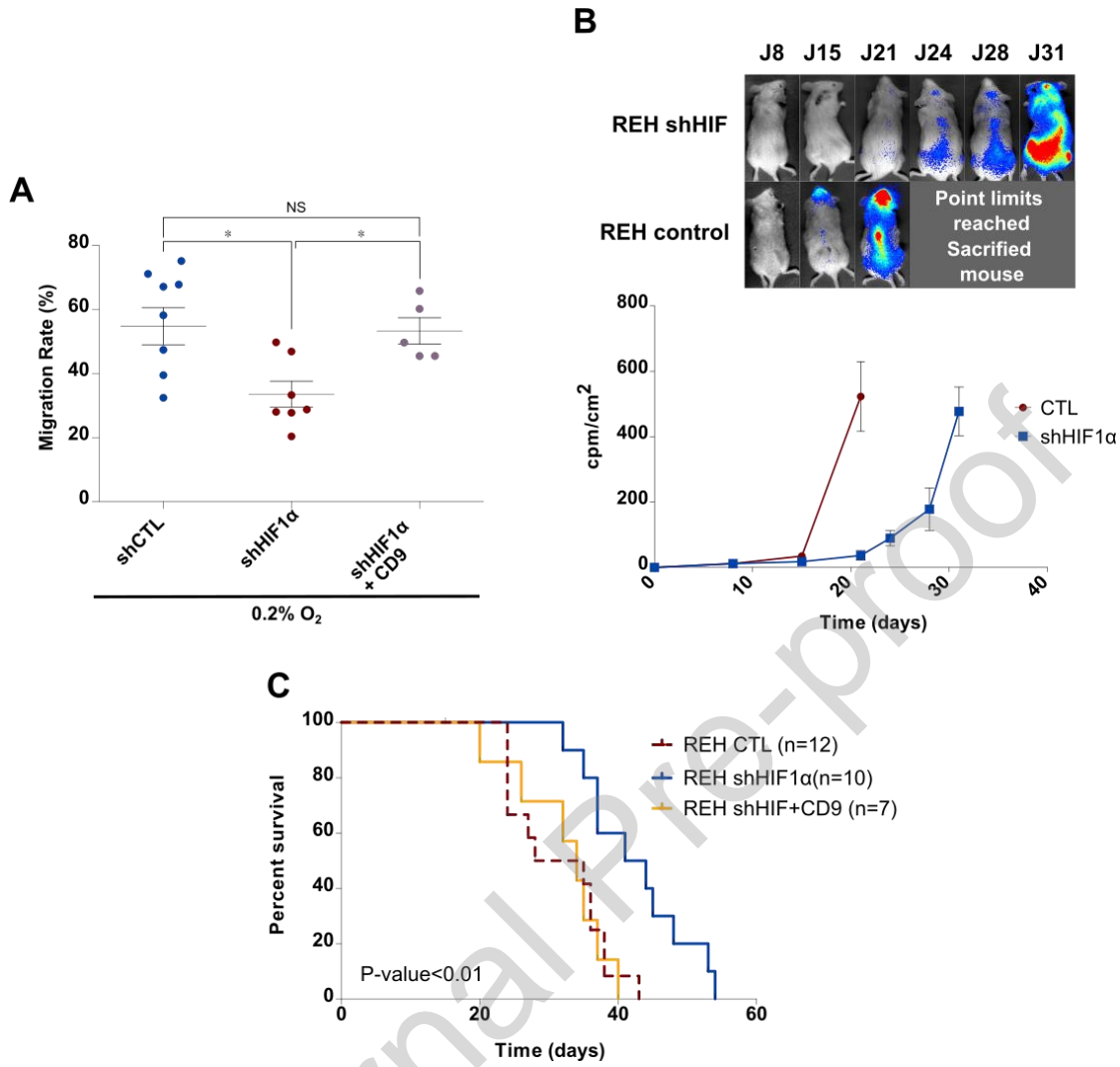
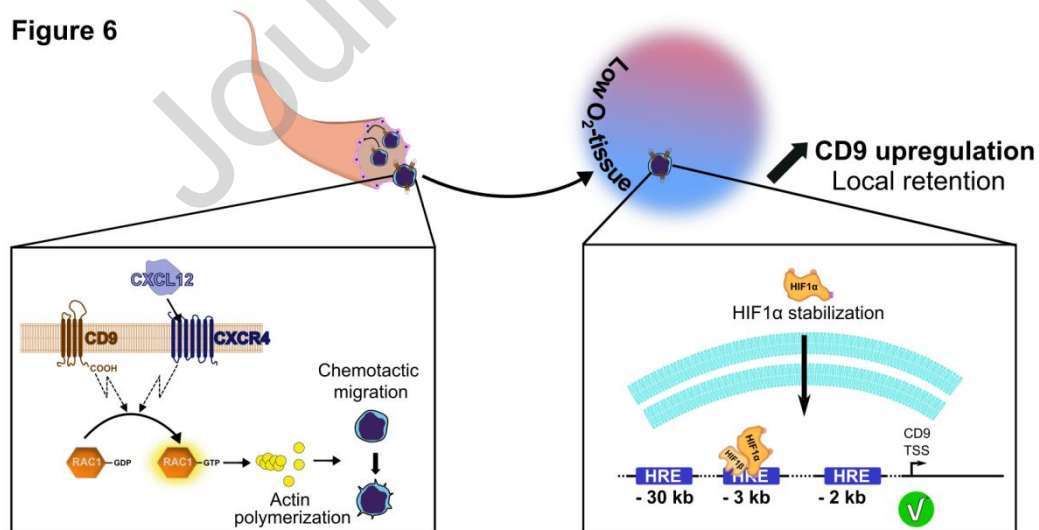


Figure 6



Disclosure of Conflicts of Interest:

The authors declare no conflict of interest. The funders had no role in the design of the study; in the collection, analyses, or interpretation of data; in the writing of the manuscript, or in the decision to publish the results.

Acknowledgments:

The authors would like to thank all the members of Gene Expression and Oncogenesis team for insightful discussions and for providing scientific expertise. We are most grateful to the patients and patients' families of the Rennes University Hospital, CHRU Rennes. We thank the following core facilities of the BIOSIT SFR UMS CNRS 3480 - INSERM 018: Mric-Photonics (Stéphanie Dutertre), flow cytometry and cell sorting (Laurent Deleurme, Gersende Lacombe), and ARCHE animal housing (Laurence Bernard-Touami), H2P2 (Alain Fautrel). We thank the MICMAC team at INSERM UMR U1236 for kindly allowing us to perform some of our experiments in their laboratory (Pr. Karin Tarte, Frédéric Mourcin).

This research was funded by the Rennes Hospital FHU CAMin (CHU de Rennes), Brittany Regional Council (Région Bretagne), comprehensive cancer Centre Eugène Marquis Cancer Care Foundation LNCC-CD35 (Ligue Contre le Cancer), Société Française de lutte contre les Cancers et leucémies de l'Enfant et de l'adolescent, Manche Leucémie association, and People Programme (Marie Curie Actions) of the European Union's Seventh Framework Programme (REA grant agreement n°291851). We are grateful to the Manche Leucémie association for their financial support.

Highlights

- Tetraspanin CD9 expression is regulated by low O₂.
- The Hypoxia Inducible Factor 1 α (HIF1 α) signaling pathway is directly involved.
- CD9-mediated migration and dissemination depends on the HIF1 α signaling pathway.